URSI GASS 2020, Rome, Italy, 29 August - 5 September 2020

Electromagnetic modelling of the SKA-LOW AAVS2 prototype

David B. Davidson*(1), Pietro Bolli(2), Mirko Bercigli(3), Paola Di Ninni(2), Jader Monari(4), Federico Perini(4), Marcin Sokolowski(1), Steven Tingay(1), Daniel Ung(1), Giuseppe Virone(5) Mark Waterson(6), Randall Wayth(1), Filippo M. Zerbi(7)
(1) ICRAR, Curtin University, Perth, WA Australia, http://astronomy.curtin.edu.au
(2) Osservatorio Astrofisico di Arcetri, Istituto Nazionale di Astrofisica, Florence, Italy
(3) Ingegneria Dei Sistemi, Pisa, Italy
(4) Istituto di Radioastronomia, Istituto Nazionale di Astrofisica, Bologna, Italy
(5) Istituto di Elettronica e di Ingegneria dell'Informazione e delle Telecomunicazioni, CNR, Turin, Italy
(6) SKA Organization HQ, Jodrell Bank, Cheshire, UK
(7) Science Directorate, Istituto Nazionale di Astrofisica, Rome, Italy

Abstract

The computational electromagnetic modelling of a large radio telescope prototype array for the Square Kilometer Array is described. The numerical models, using the Method of Moments, are characterised by a very large number of unknowns, requiring the use of fast solution methods and high performance computing platforms. Good agreement has been obtained between results obtained on two different commercial codes. Results for both embedded element patterns and the station beam are shown. The use of the computed embedded element patterns for array calibration is briefly addressed.

1 Introduction

The Square Kilometre Array (SKA) project is an international effort to build the world's largest radio telescope [1], with an eventual collecting area of a square kilometre. It it split between the SKA-MID dish array, sited in South Africa, and the SKA-LOW aperture array, sited in Western Australia. 2019 saw the signing of the intergovernmental SKA Observatory (SKAO) treaty, currently being ratified by the initial signatory states, and the close-out of the System Critical Design Review at year end.

Work in Australia and Italy is currently focussed on the deployment, simulation, measurement, calibration and commissioning of new low-frequency aperture array prototype stations for SKA-LOW, with nominal frequency coverage 50–350 MHz. The latest is the Aperture Array Verification System (AAVS) Version 2. A recent paper outlined earlier prototypes [2].

The authors have extensively investigated the pattern characteristics of wide-band antennas operating in highly-coupled electromagnetic environments during the development of the SKA-LOW design proposals and this work represents the latest in this line. The primary objective of this effort is to derive and validate embedded element patterns (EEPs) which can be used in calibration calculations, and to understand the limitations and errors in these models. In the following sections, this paper describes the electromagnetic modelling required to compute the antenna embedded element patterns.

2 The AAVS2 Prototype

The AAVS2 (also known as AAVS2.0) verification system consists of an array of 256 dual-polarized log-periodic SKALA4.1 antennas, distributed on a wire-mesh ground plane. More details on this antenna may be found in [2]. The maximum centre-centre distance between antennas is 38 m and the array layout is semi-random; some antenna positions have been fine-tuned to avoid mechanical interference and a reasonable walk-through to access every antenna. The demonstrator was deployed at the Murchison Radio-astronomy Observatory (MRO) site during the course of 2019; a picture of the completed array is shown in Fig. 1. One of the main drivers behind its construction was to address the issue of array calibratability. Two single-ended 50-ohm Low Noise Amplifiers are fully integrated in each antenna and are connected through coaxial cables (10-m long) to a box where the RF signals are pre-conditioned and converted for transmission via optical fibers to the central processing unit.

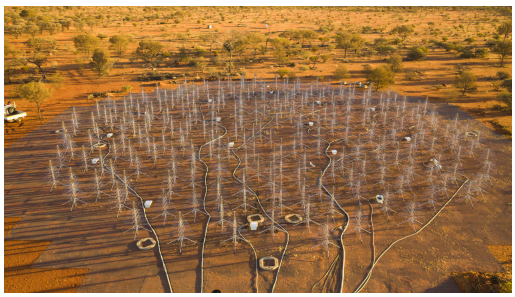

Figure 1. An aerial side view of the AAVS2 array, November 2019. Credits: ICRAR/INAF.

3 Numerical modelling of the array

For modelling the highly-conducting SKALA4.1 antennas, the Method of Moments (MoM) is a very competitive method. Only the radiating surface is meshed, or discretized (i.e. modelled with small surface or wire elements). In both the Finite Difference Time Domain and the Finite Element Methods, the whole three-dimensional volume containing the antenna must be meshed with volume-based elements, and an additional volume around this must also be meshed, to allow some type of radiation boundary condition (or more generally, some form of mesh closure scheme) to be applied. Most MoM codes, including FEKO and Galileo-ElectroMagnetic Toolkit, the two used in this work, use a linear element to approximate the electric current along a wire filament, and a mixed order element defined on a triangle to approximate surface current. The latter was first published in the 1980s, and is widely known as the RWG element after the initials of its originators [3].

The main results needed from the simulations are the set of embedded element patterns and the array mutual coupling matrix, or equivalently, the S-parameters of the full array. For the dual-polarised SKA-LOW stations, there are 512 co-polarised EEPs (sampled over the upper hemisphere, typically with an angular resolution of one degree); the $[Z]$, $[Y]$ or $[S]$ matrix size is 512×512. The EEPs have to be computed one at a time, as loading conditions are applied to all other ports other than the driven one. Here, matched loads have been applied [2].

A prime consideration when modelling antenna arrays as complex as the AAVS antenna system is to generate a mesh which is sufficiently fine to adequately resolve the current distribution — but no finer, as the computational cost grows very rapidly. The MoM in its standard form has a memory requirement which grows as $\mathcal{O}(N^2)$, and computational cost which grows as $\mathcal{O}(N^3)$. N is the number of mesh elements, or degrees of freedom, and for a thin-wire antenna is proportional to frequency. For electromagnetically large problems, the Fast Multipole Method (FMM), originally introduced in the mid-1980s to speed up the calculation of long-range forces in the n-body problem, was adapted to the iterative solution of MoM problems in the early 1990s [4]; combined with major advances in high-performance computing, it has proven key to solving very large problems. In its multi-level form, the MLFMM (also known as MLFMA) method has an asymptotic computational dependence of $\mathcal{O}(N \log N)$ per iteration. Unfortunately, the iterative solver is not guaranteed to converge, and this becomes particularly problematic for low frequency problems, where convergence can be very slow or even absent. Nonetheless, the MLFMM has become the standard for the discrete (i.e. meshed) solution of Maxwell's equations in integral form. FEKO was the first commercial code to include the MLFMM (circa 2000); many commercial MoM packages now include an implementation.

Due to the increased number of dipoles on each arm comprising the log-periodic structure compared to previous prototypes, the SKALA4.1 is appreciably more complex to model numerically than its predecessor in AAVS1, the SKALA2, not least in terms of the use of solid metal elements at the high-frequency end. FEKO and Galileo models have been developed that retain sufficient fidelity to accurately predict input impedance across the frequency range of interest, whilst simplifying some of the geometrical features of the as-built structure. This has been discussed in [2]. Even after further simplification of the MoM models, the numerical models typically comprise well over a million degrees of freedom (N) for the full 256 antenna station. Run-times per frequency point vary from days to weeks, depending on the convergence rates of the iterative solver used for the MLFMM solution, even on powerful dedicated servers. FEKO simulations at Curtin have been carried out on a DEC PowerEdge 740 server, with dual Xeon Platinum 8180 processors providing a total of 56 cores and with 1.5 TB of RAM available. FEKO supports parallel processing for the MLFMM. In CEM language, EEP computation is a "multiple right-hand-side (RHS) " problem [5]. If the resulting $N \times N$ matrix equation could be solved using a direct method, subsequent RHSs can be rapidly solved — however, direct solutions are not viable for this number of unknowns. The MLFMM is an iterative technique, so has to restart the solution for each EEP. This is a major and unavoidable factor contributing to these very long run-times. Similar considerations on the EM modelling of AAVS2 apply also for the commercial CEM software suite Galileo, which also offers MLFMM acceleration.

It is worth noting that in both FEKO and Galileo models, an infinite perfect metallic conductor plane is implemented under the array to model the mesh ground plane.

Promising work continues on alternative approaches to fast solvers. An example is HARP [6], based on extensions to a macro-basis function approach [7]. However, this method has not been implemented to date in commercial codes. Another is the Domain Green's function approach [8]; FEKO supports an implementation of this, but unfortunately it is not well suited to the computation of EEPs.

4 Numerical results

4.1 Embedded Element Patterns

Comparative results for FEKO and Galileo are shown in Fig. 2. Antenna 2 is located 17.7 m east and 3.94 m south of the station centre; it lies towards the periphery of the station. E-plane and H-plane have their usual meanings; for dual polarized antennas such as these, it refers to one polarisation. Here, for both arrays the results are for the X (east-west) arm. Due to the symmetry in the antennas, results for X and Y should be broadly similar, although not identical, since the quasi-random station is not symmetrically laid out. In general, the agreement is generally good, although some EEPs show more inter-code variation in the

case of AAVS2 than was the case for the smaller AAVS1.5 array, for which results were shown in [2]. One reason for this is that MoM models had to be further simplified to permit them to run at all. It will be noted that the EEPs are not symmetrical; this is due to mutual coupling in the array, which is captured in the EEP. A detailed analysis of the variation exhibited by EEPs was reported in [2] for the initial 48 element deployment (which grew into the full 256 element AAVS2).

4.2 Array Pattern

Figure 3 shows a comparison of the zenith-pointing station beams, E-plane, synthesized from the computed EEPs. As expected, the pattern for AAVS2 is much better in terms of the first and second sidelobes than that shown for the earlier AAVS1.5 [2, Fig. 6]. The first sidelobe is at approximately -17 dB, consistent with a uniformly illuminated circular aperture. As expected from the quasi-random element distribution, the far-out sidelobe structure is of the order of $\frac{1}{N}$ down in terms of power (approximately -24 dB) [7]. Some differences in the positions of far-out nulls are visible; these are at very low relative power levels.

5 Conclusions

With this work, we have been able to demonstrate excellent agreement between simulated patterns for an electromagnetically very large array. This has been possible by leveraging fast algorithms available in commercial codes, supporting parallel execution on powerful multi-core workstations, and by developing suitably simplified models of the individual array elements, viz. the SKALA4.1 antenna.

A drone campaign was undertaken following the initial rollout of this array (the 48 element AAVS1.5). Results have been reported in [9] showing an excellent agreement between simulations and measurements. However, the simulation and measurement of the embedded element patterns is not an end in itself; the key question still to be addressed is whether the significant variation in element patterns, caused by mutual coupling, will permit sufficiently accurate and rapid station-level calibration for SKA-LOW. The inter-element variability is especially pronounced at the lower end of the frequency band. Existing calibration scheme generally assume that all the EEPs are similar, and it is clear that this is not the case. Recent work on this is reported in [10] and work on this continues.

6 Acknowledgements

David Davidson and Pietro Bolli are co-first authors.

AAVS2 is hosted by the MWA under an agreement via the MWA External Instruments Policy. This scientific work makes use of the Murchison Radio-astronomy Observatory, operated by CSIRO. We acknowledge the Wajarri Yamatji people as the traditional owners of the Observatory site.

References

[1] P. E. Dewdney, P. J. Hall, R. T. Schilizzi, and T. J. L. W. Lazio, "The Square Kilometre Array," *Proceedings of the IEEE*, vol. 97, no. 8, pp. 1482–1496, Aug 2009.

[2] D. B. Davidson, P. Bolli, M. Bercigli, P. di Ninni, R. Steiner, S. Tingay, D. Ung, A. van Es, G. Virone, and R. Wayth, "Electromagnetic modelling of the SKA-LOW AAVS1.5 prototype," in *2019 International Conference on Electromagnetics in Advanced Applications (ICEAA)*, Sep. 2019, pp. 1032–1037.

[3] S. Rao, D. Wilton, and A. Glisson, "Electromagnetic scattering by surfaces of arbitrary shape," *IEEE Transactions on Antennas and Propagation*, vol. 30, no. 3, pp. 409–418, May 1982.

[4] R. Coifman, V. Rokhlin, and S. Wandzura, "The fast multipole method for the wave equation: a pedestrian prescription," *IEEE Antennas and Propagation Magazine*, vol. 35, no. 3, pp. 7–12, June 1993.

[5] D. B. Davidson, *Computational Electromagnetics for RF and Microwave Engineering*, 2nd ed. Cambridge, UK: Cambridge University Press, 2011.

[6] H. Bui-Van, J. Abraham, M. Arts, Q. Gueuning, C. Raucy, D. González-Ovejero, E. de Lera Acedo, and C. Craeye, "Fast and accurate simulation technique for large irregular arrays," *IEEE Transactions on Antennas and Propagation*, vol. 66, no. 4, pp. 1805–1817, April 2018.

[7] K. F. Warnick, R. Maaskant, M. Ivashina, D. B. Davidson, and B. Jeffs, *Phased Arrays for Radio Astronomy, Remote Sensing, and Satellite Communications*. Cambridge, UK: Cambridge University Press, 2018.

[8] D. J. Ludick, R. Maaskant, D. B. Davidson, U. Jakobus, R. Mittra, and D. de Villiers, "Efficient analysis of large aperiodic antenna arrays using the domain Green's function method," *IEEE Transactions on Antennas and Propagation*, vol. 62, no. 4, pp. 1579–1588, April 2014.

[9] F. Paonessa, L. Ciorba, G. Virone, P. Bolli, A. Magro, A. McPhail, D. Minchin, and R. Bhushan, "First results on the validation of the SKA-Low prototypes using an airborne test source," in *XXXIII General Assembly and Scientific Symposium (GASS) of the International Union of Radio Science (URSI)*, Aug. 2020.

[10] S. J. Wijnholds, M. Arts, P. Bolli, P. di Ninni, and G. Virone, "Using embedded element patterns to improve aperture array calibration," in *2019 International Conference on Electromagnetics in Advanced Applications (ICEAA)*, Sep. 2019, pp. 0437–0442.

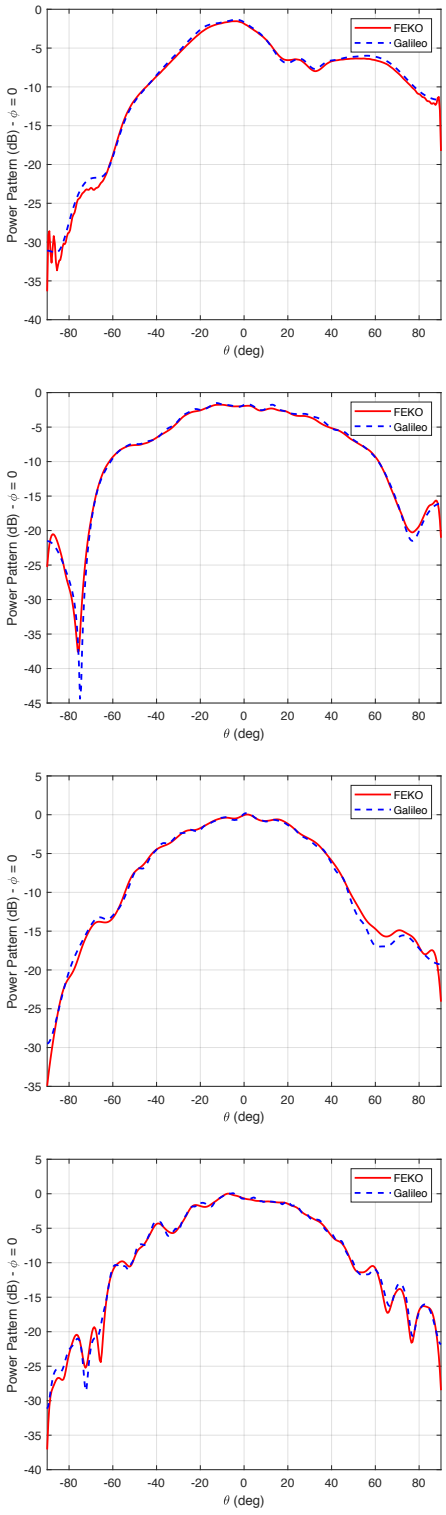

Figure 2. A comparison of EEPs for antenna number 2 computed using FEKO and Galileo for AAVS2. Top to bottom: 80, 110,160 and 350 MHz. EW (X) polarization.

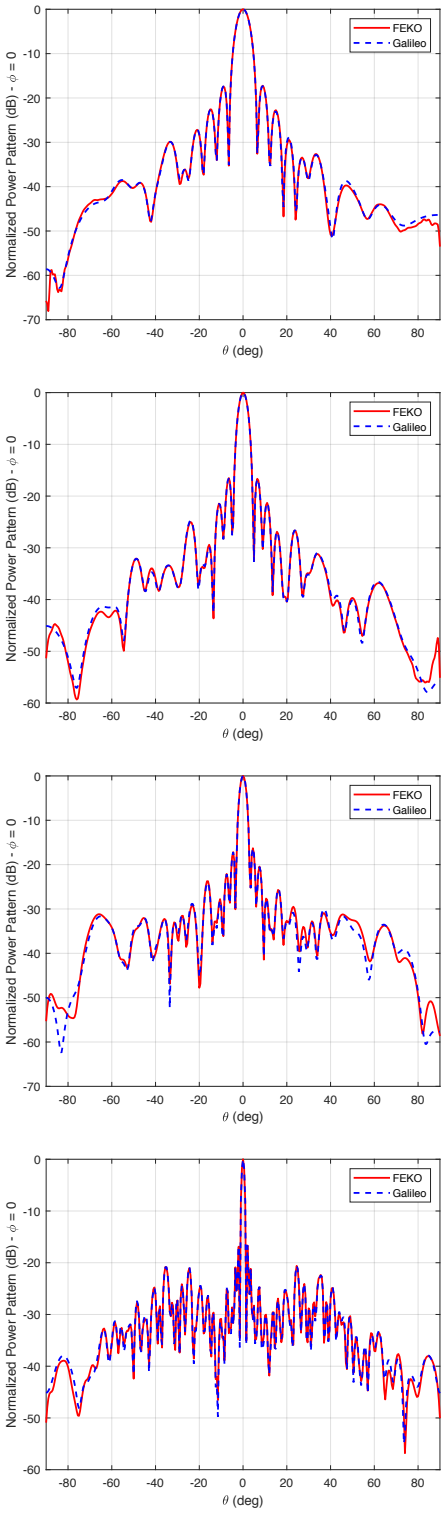

Figure 3. E-plane zenith pointing station beams for the 256 element AAVS2 station. Top to bottom: 80, 110, 160 and 350 MHz. EW (X) polarization.